Association of Metallurgical Engineers of Serbia *Scientific paper*
AMES *UDC: 620.17:669.715'55*

EFFECT OF IMPURITIES ON MICROSTRUCTURE OF THE AS-CAST AND HEAT TREATED AL-ZN ALLOYS

Douniazed Lamrous[1*], Emanuelle Boehm-Courjault[2], Mohamed Y. Debili[1], Nacira Sassane[1]

[1]*Laboratory of Magnetism and Spectroscopy of Solids, Physics Department, Faculty of Science, Badji-Mokhtar -Annaba University, 23200 Annaba, Algeria, mydebili@yahoo.fr*
[2]*Computational Materials Laboratory, Ecole Polytechnique Fédérale de Lausanne, Station 12, Lausanne CH-1015, Switzerland*

Received 21.10.2013
Accepted 12.11.2013

Abstract

The microstructure of two Al-Zn alloys (with 10 and 30 wt.%Zn content) produced by melting in the high frequency induction furnace were investigated by means of scanning electron microscopy (SEM), energy dispersive X-ray (EDX) spectroscopy, X-ray diffraction (XRD) analysis and the microhardness tests. The results indicate that the presence of iron impurity causes the formation of eutectic $(Al,Zn)_3Fe$ in both alloys. The presence of the silicon impurity results in the formation of the phase separation in the Al-10%Zn as-cast alloy. The columnar to equiaxed transition was produced only in the Al-30%Zn as-cast alloy. The Vickers microhardness is higher in the equiaxed zone than in the columnar to equiaxed transition (CET) zone. The presence of iron causes intermetallic phase formation $(Al, Fe, Si)_{3,6}Zn$ in the Al-30%Zn as-cast alloy enabling an increase in the lattice parameter. After a homogenization treatment, the microstructure of Al-Zn treated alloys consists only of α dendrites and stable eutectic phase.
Keywords: Al-Zn, HF melting, Dendrites, CET, Impurities, Structural properties.

Introduction

Iron and silicon are common impurities in aluminium and its alloys and may cause adverse effects to microstructure and structural properties. The solid solubility of iron in aluminium is very low with the result that most iron forms intermetallic compounds, the nature of which strongly depends on other present impurities or alloying elements [1-3]. Silicon does not form compounds with aluminium, it was

* Corresponding author: Douniazed Lamrous, dlamrous@yahoo.fr

shown that the presence of iron in the Al-Si causes a change of the microstructural properties [4], giving rise to the formation of intermetallic phases.

Aluminium can form solutions of variable solubility, when melted together with many elements such as zinc, silicon, copper, magnesium, zirconium and some others.

The dendritic structure which is the most common microstructure developed during solidification of metallic alloys, can be either columnar or equiaxed and also the transition from a columnar to equiaxed (CET) microstructure is possible to occur. All these types of microstructures could be found in Al-Zn alloys [5]. In these alloys α solid solution based on aluminium which can dissolve up to 83 wt.%Zn, may decompose in a definite interval of temperatures and concentrations into two solid solutions of the same crystal structure: one rich in zinc and other low in zinc content.

The objective of the present investigation was to study the effect of iron and silicon impurities on microstructure of as-cast and treated Al-Zn alloys.

Experimental Procedure

Two aluminium-zinc alloys (Al-10 wt.%Zn and Al-30 wt.%Zn) were prepared from pure Al (99%), pure Zn (99.99%) and melted by high frequency induction fusion (HF) Linn Therm 600 type (6 KW, 300 KHz) furnace under the primary vacuum of 10^{-2} torr. Cold compaction of blended powder was carried out to obtain a dense product intended for high frequency induction fusion. The microstructure of the alloys was examined on metallographic microsections. Mechanical polishing technique (600-4000 SiC grinding paper and polishing cloth with 6, 1 and 0.25 μm then 0.03μm colloidal silica) was used to prepare the transverse sections for scanning electron microscope (SEM), (FEI XL30 SFEG Philips), under the accelerating voltage of 15 kV. The samples were etched for 15 s with Keller's reagent (5 ml HF+9 ml HCl+22 ml HNO_3+74 ml H_2O). Chemical composition of phases present in these alloys was measured using energy dispersive X-ray spectrometry X (EDS), (Thermo Electron Corporation), equipped with Noran System Six software. Identification of the phases was carried out using an x-ray diffractometer operated at Cu Kα radiation, with diffraction angle (2θ) from 20° to 90°. Microhardness (Hv) was measured on at least 8 different regions on tranverse sections using a 200 g load and a dwell time of 30 s.

The samples were subjected to a homogenisation heat treatment in a vacuum furnace working under a pression of 10^{-2} torr . They were heated at 500°C and homogenized during 1 h, then air-cooled.

Results and Discussion

Figure 1(a) shows the presence of two zones in Al-10%Zn as-cast alloy. The separation interface between the two zones consists of a precipitate- free region. Figure 1 (b) illustrates a typical SEM micrograph showing the existence of this separation interface with an average width around 20 μm. The corresponding X(EDS) measurements reveal the presence of aluminium, zinc and silicon (Table 1).

Table 1. X (EDS) chemical analysis of interface of Al-10%Zn alloy.

Wt. %	***Al***	***Zn***	***Si***
Point 1	76.8	12.2	4.5
Point 2	77.7	12.4	3.1
Point 3	78.1	13.0	2.3

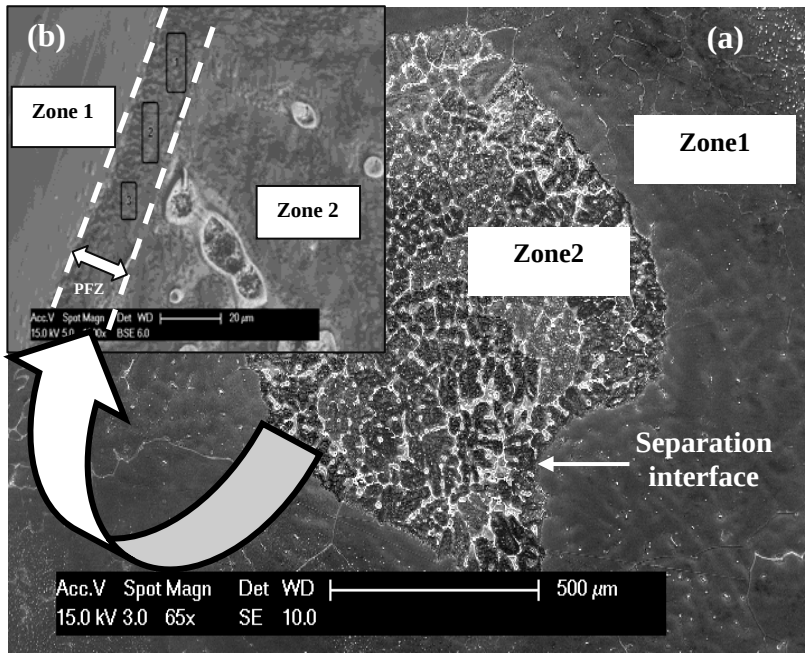

Figure 1. a) SEM-SE micrograph of a transverse section of Al-10%Zn as-cast alloy, b) SEM-BSE image of interface between α and α' phases.

As can be seen from Figure 2, the microstructure of the zone 1 consists of α-Al dendrites and eutectic in interdendritic regions. The X(EDS) chemical analysis carried out on eutectic bright lamellae from Figure 3, confirms that they are composed of aluminium, zinc and iron (Table 2). The iron impurity presence in Al-Zn alloy do not dissolve but crystallises as intermetallic compound [6, 9] forming a ternary compound $(Al, Zn)_3$ Fe, which is a part of a regular eutectic of α-Al phase.

Table 2. X (EDS) chemical analysis of eutectic bright lamellasof Al-10%Zn alloy.

Wt. %	***Al***	***Zn***	***Si***
Average values	67.2	8.1	24.7

Table 3. X (EDS) chemical analysis of α-Al phaseof Al-10%Zn alloy.

Wt. %	***Al***	***Zn***	***Si***	***Fe***
Point 5	94.0	5.6	0.2	0.2
Point 6	93.9	5.6	0.2	0.3
Point 7	93.2	6.4	0.2	0.2

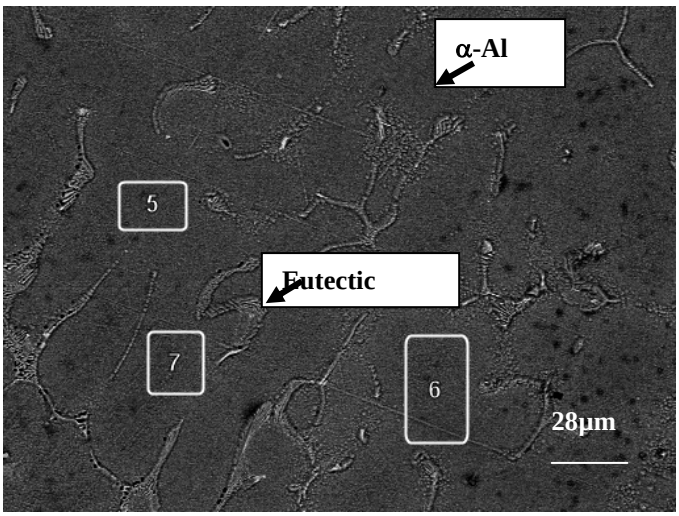

Figure 2. SEM micrograph indicating the zones (5, 6, 7) where EDX measurements of Table 3 were done.

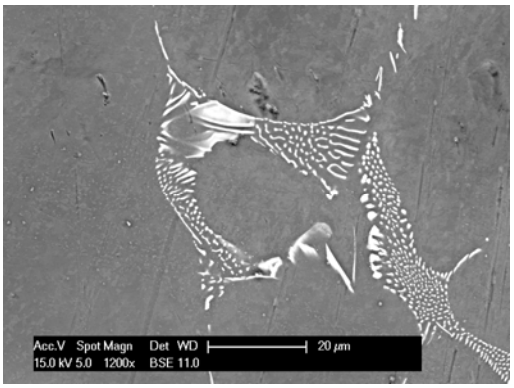

Figure 3. SEM -BSE micrograph showing eutectic morphology.

The microstructure of the zone 2 is formed from: dendrites, precipitates and a clear grey phase around precipitates. The diffraction lines (111) and (311) show a separation into side-bands (Figures 5a and 5b). Analyses carried out on the α-Al matrix (Figure 2 and Table 3), showed that it contains 6 wt.% of zinc. The analyses performed on the α'-Al dendrites (Figure 4), summarized in Table 4, show that they are zinc-rich (23 wt.%Zn).

Figure 6 represents plots of concentration profiles of silicon and iron throughout α/interface/α'; the iron concentration remains nearly constant and close to 0%, while silicon concentration is at its maximum. These results revealed the role of silicon impurity on the phase separation. It was observed in the Zn–40Al–2Cu–(0.5–5)Si

alloys, when the silicon content exceeded the 2.5% level, silicon particles gave rise to micro-segregation in the alloys by gathering in some areas as separate groups [7].

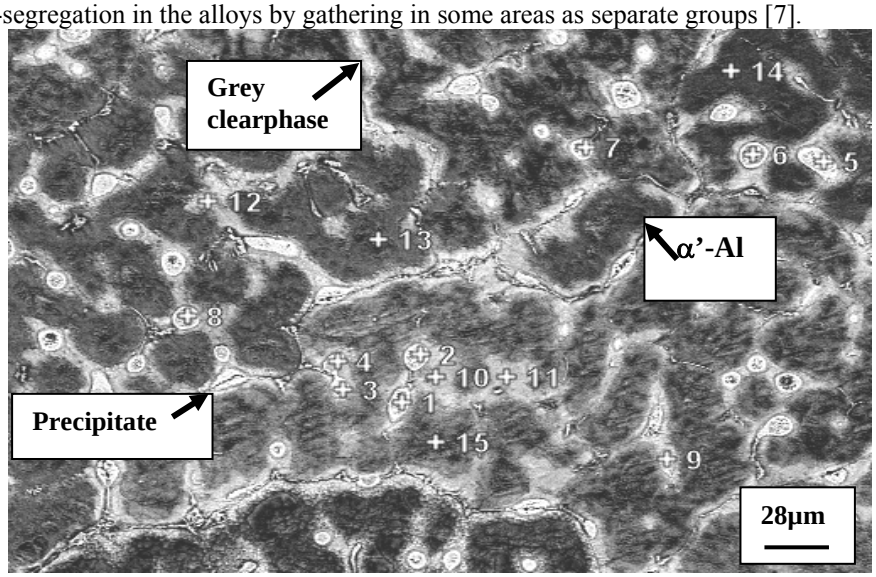

Figure 4. SEM micrograph showing the analysed points correspondingto precipitates and α' phase (the EDX composition resultsof points 1 to 15 are given in Tables 4, 5 and 6).

X(EDS) chemical analyses of precipitates present in Figure 4 shows that all particles belong to a phase consisting of aluminium, zinc and silicon (Table 5). Chemical analyses from points 10 to 12 (Figure 4), performed on the clear grey phase surrounding precipitates, is included in Table 6. It was noticed that this phase has a composition close to that of the precipitates. It was previously reported that silicon causes the formation of precipitates [8].

Table 5. X (EDS) chemical analysis ofnine precipitatesof Al-10%Zn alloy.

Wt. %	***Al***	***Zn***	***Si***	***Fe***
Point 1	69.3	28.9	1.8	0.0
Point 2	66.4	33.2	0.2	0.2
Point 3	69.1	28.8	1.9	0.2
Point 4	72.7	26.4	0.7	0.2
Point 5	67.2	31.1	1.7	0.0
Point 6	66.7	33.0	0.3	0.0
Point 7	69.4	29.4	1.2	0.0
Point 8	63.8	35.3	0.7	0.2
Point 9	69.3	27.8	2.9	0.0

Table 6.X (EDS) chemical analysis of areaaround precipitatesof Al-10%Zn alloy.

Wt. %	***Al***	***Zn***	***Si***	***Fe***
Point 10	66.4	32.5	1.0	0.1
Point 11	69.4	30.2	0.3	0.1
Point 12	70.3	27.9	1.7	0.1

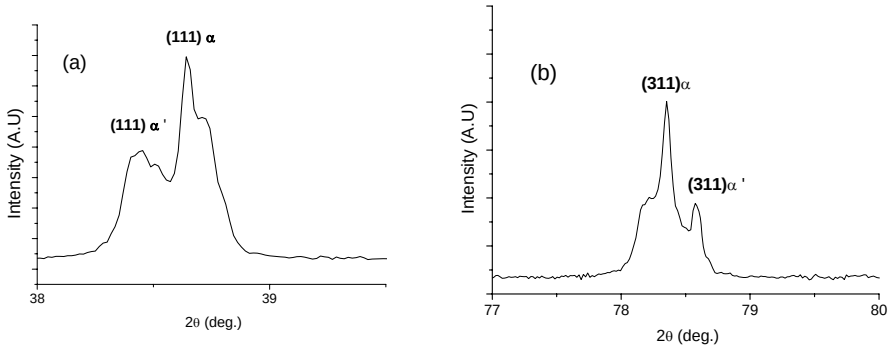

Figure 5. a, b) X-ray diffraction lines of (111) and (311) planes of Al-10%Zn as-cast alloy.

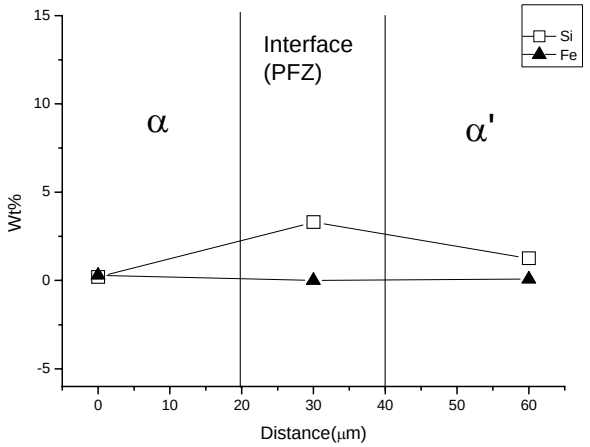

Figure 6. Concentration profile throughout α/interface/α' versus distance.

The columnar to equiaxed transition (CET) which was a consequence of the hydrodynamic flow of liquid in contact with columnar dendrite, was observed in Al-30%Zn as-cast alloy (Figure 7). The size of dendrites is 55 μm, and for the equiaxed grains is 22 μm.

Microstructural SEM investigations (Figures 8, 9) show that this alloy contains precipitates and intermetallic phase. The composition of precipitates is close to that of the Al-10%Zn alloy (Table 7).

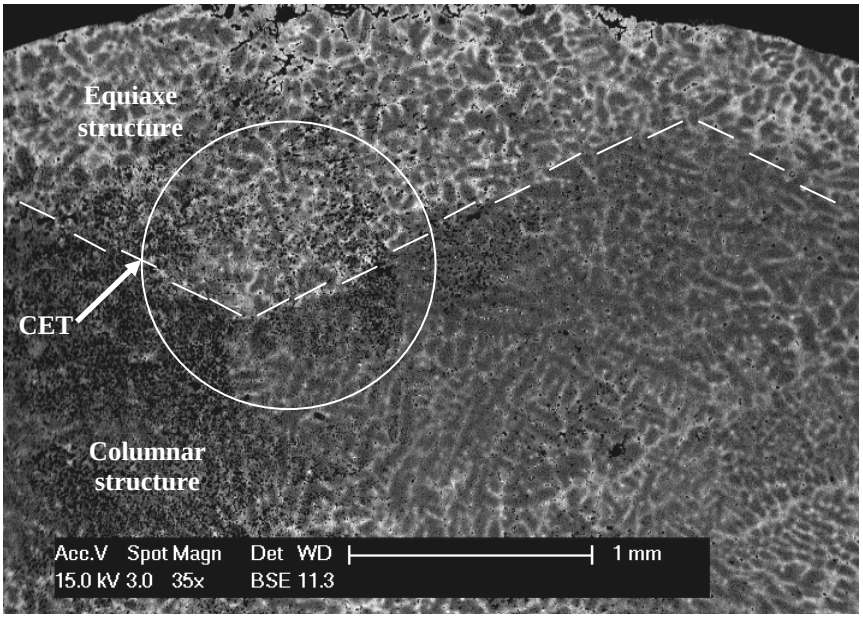

Figure 7. Global image of a transverse section of Al-30%Zn as-cast alloy.The CET zone, when present, is indicated by the broken dotted white lines.

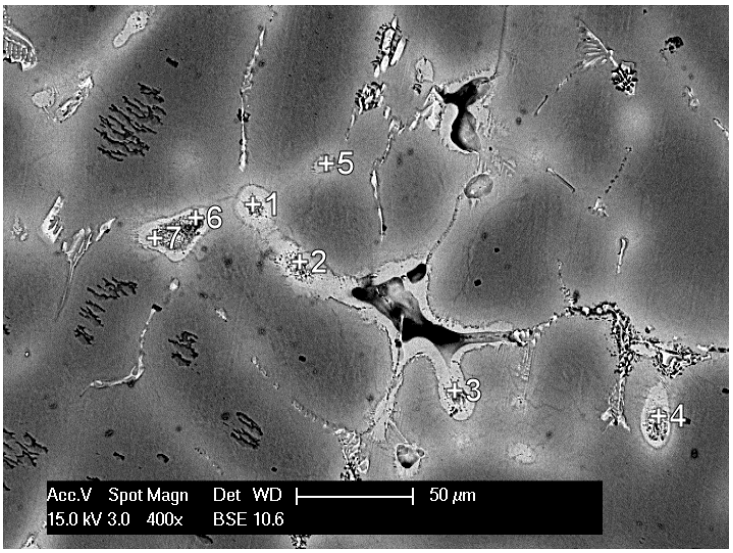

Figure 8. SEM micrograph of the Al-30%Zn as-cast alloy showing analysed points corresponding to precipitates.

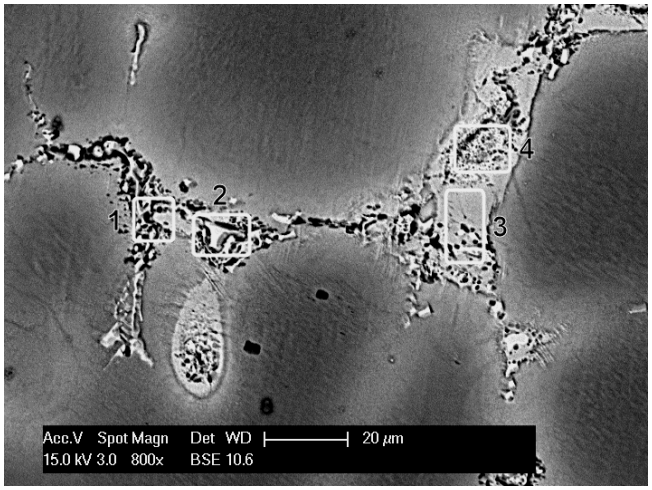

Figure 9. SEM-BSE micrograph of Al-30%Zn as-cast alloy of analyzed surfaces corresponding to intermetallic phase.

Table 7. X (EDS) chemical analysis of precipitates of Al-30%Zn alloy.

Wt. %	***Al***	***Zn***	***Si***	***Fe***
Point 1	59.7	40.0	0.3	0.0
Point 2	60.6	38.9	0.3	0.2
Point 3	61.1	38.4	0.2	0.3
Point 4	64.1	35.3	0.3	0.0
Point 5	65.7	33.9	0.3	0.1
Point 6	64.1	35.6	0.2	0.1
Point 7	59.6	39.8	0.5	0.1

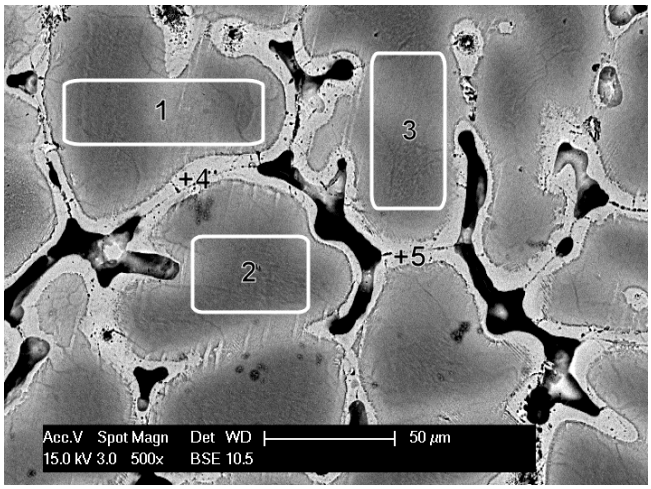

Figure 10. SEM-BSE micrograph of Al-30%Zn as-cast alloy of analyzedsurfaces and points corresponding to the matrix and clear grey phase.

Chemical composition of the matrix of Al-10%Zn alloy (Figure 10) was analyzed by X(EDS) and the results are given in Table 8. It can be seen from Figure 10, that the matrix appears dark grey with respect to a phase present in the interdendritic spacing. Apparently, there is no difference in the composition (Table 9) of the clear grey phase in these two alloys.

Table 8.X (EDS) chemical analysis of the matrix of Al-30%Zn alloy

Wt. %	***Al***	***Zn***	***Si***	***Fe***
Area 1	75.0	24.7	0.1	0.2
Area 2	78.0	21.9	0.1	0.0
Area 3	74.4	25.3	0.2	0.1

Table 9. X (EDS) chemical analysis of areaaround precipitatesof Al-30%Zn alloy

Wt. %	***Al***	***Zn***	***Si***	***Fe***
point 4	59.5	40.0	0.4	0.1
point 5	62.7	36.8	0.4	0.0

The results of XRD analysis in the form of diffractogram is shown in Figure 11. Combination of X(EDS) and XRD results allow us to identify the intermetallic phase as a $(Al,Si,Fe)_3Zn$ (Table 10) and the precipitates as δ- Al_9FeSi_3 phase.

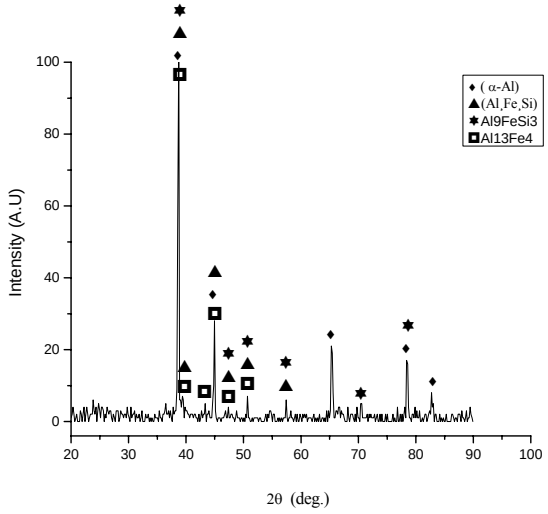

Figure 11. X-ray diffraction patterns of Al-30%Zn as-cast alloy.

Table 10.X (EDS) chemical analysisof intermetallic phaseof Al-30%Zn alloy

Wt. %	***Al***	***Zn***	***Si***	***Fe***
Area 1	60.1	37.7	0.4	1.8
Area 2	54.9	27.8	2.8	14.5
Area 3	59.3	36.7	0.0	4.0
Area 4	54.4	42.2	1.0	2.4

After a homogenization treatment at 500°C for 1 h, the microstructure of Al-10%Zn, Al-30%Zn alloys is shown in Figures 12 and 13, respectively. In both alloys the microstructure mainly consists of the α-Al phase and eutectic. The α'-Al phase, the precipitates and the intermetallic phase were disappeared, proving the non-equilibrium character of these alloys. The eutectic remains present because its melting temperature is around 655°C.

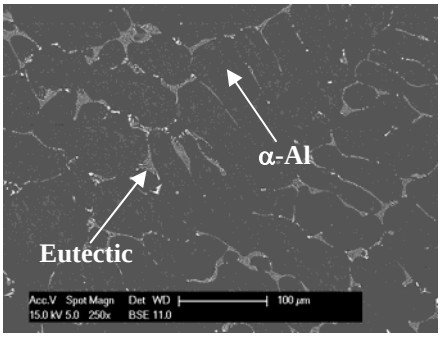

Figure 12. SEM-BSE micrograph of homogenized Al-10%Zn alloy.

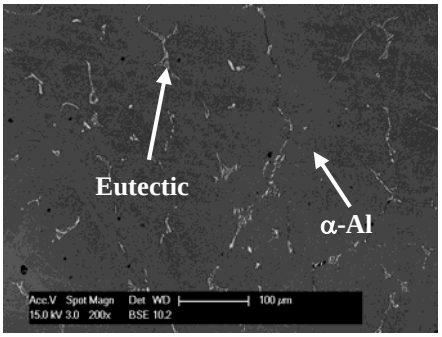

Figure 13. SEM-BSE micrograph of homogenized Al-30%Zn alloy.

The lattice parameter of the as-quenched Al-Zn alloys, a (α-Al), in dependence on the zinc composition is shown in Figure 14. These values indicate that the lattice parameter of the α-Al phase of the Al-10%Zn was in a fair agreement with the data given in the literature [10-13]: a(α-Al) decreased linearly with the increase of zinc content. On the other side, the unit-cell parameter, a(α-Al), of the Al-30%Zn alloy was found to increase. This behavior may be explained by the iron impurity presence which formed intermetallic compounds. Iron has a very low solubility in the solid, and tends to combine with other elements to form intermetallic phase particles of various types. It was observed that the presence of iron in the Al-Si alloy causes a slight increase in the lattice parameter [4], enabling more intermetallics to be formed and hence more unconstrained growth is able to occur.

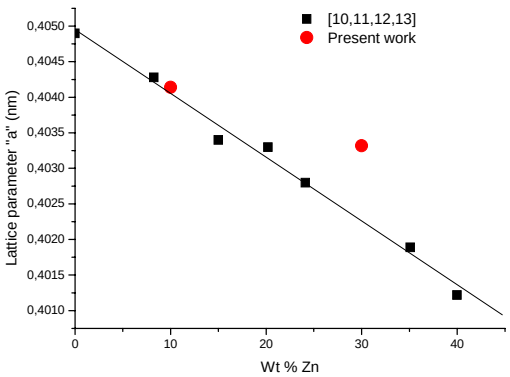

Figure 14. Lattice parameter variation versus of Zn content of as-cast Al-Zn alloys.

Figure 15 shows experimental results of microhardness variations analyses as a function of zinc concentration, for as-cast and homogenized alloys. The Al-30%Zn as-cast alloy has higher hardness due to the presence of higher concentration of intermetallic phase(Al, Fe, Si)$_{3,6}$Znbeing much harder than the remainder of the alloy. The microhardness is greater in the equiaxed zone (95 Hv) than in the columnar to equiaxed transition (CET) zone (76,5 Hv). Also, we determined that the grain size decreases from the columnar to the equiaxed structure. Regarding to this, the values of the microhardness increase with the decreasing values of grain size, which is in accordance with the Hall-Petch effect.

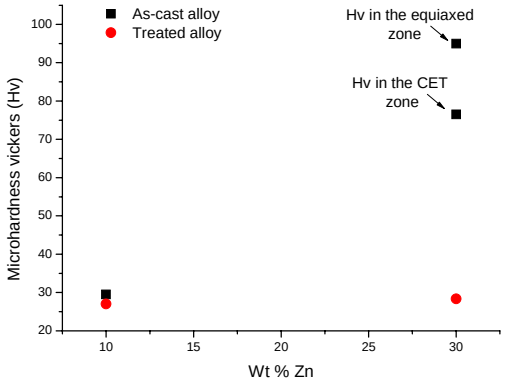

Figure 15. Microhardness variation versus of Zn content of as-cast and treated Al-Zn alloys.

After a homogenized heat treatment, the microhardness decreases in the Al-30%Zn alloy treated because the intermetallic phase was disappeared. It can be seen that the microhardness variation is not sensitive to composition.

Conclusion

The following remarks can be drawn from the results of the present investigation:

- Iron and silicon impurities have different effects on the microstructure of Al-Zn alloys produced in high frequency induction furnace.
- The phase separation was observed in the Al-10%Zn as-cast alloy and the microstructureconsists of α-Al (rich in zinc content), α'-Al (low in zinc content), precipitates and eutectic.
- All precipitates consist of aluminium, zinc and silicon. Silicon causes the appearance of precipitates and phase separation.
- The columnar to equiaxed transition is produced in the Al-30%Zn as-cast alloy, its microstructure consist of α-Al, precipitate, eutectic and intermetallic phase (Al,Fe,Si)$_{3,6}$Zn.
- Iron causes the formation of eutectic (Al,Zn)$_3$Fe.
- The microhardness is greater in the equiaxed zone (95Hv) than in the columnar to equiaxed transition (CET) zone (76,5Hv).
- The microhardness of the Al-30%Zn as-cast alloy is higher than that of the Al-10%Zn as-cast alloy.

- The microhardness increases with decreasing grain size in accordance with Hall-Petch effect.

- The presence of iron causes intermetallic phase formation in the Al-30%Zn as-cast alloy enabling an increase in the lattice parameter.

- The microstructure of Al-Zn homogenized alloys consists only of α dendrites and stable eutectic phase.

-The microhardness decreases in Al-30%Zn homogenized alloy when intermetallic phase $(Al,Fe,Si)_{3,6}Zn$ disappear.

Acknowledgment

All observations by SEM and X (EDS) were carried out with Electronic Microscopy interdisciplinary center of EPFL (Ecole Polytechnique Fédérale de Lausanne), in collaboration with Computational Materials Laboratory of EPFL. We are gratefully acknowledged to the staff.

References

[1] P. L. Mangonon, P. E. Fasm, In: Prentice-Hall International, Inc, The principles of Materials Selection for Engineering Design 1999, p. 560.
[2] N.A. Belov, A.A. Aksenov, Iron in Aluminium Alloys: Impurity and Alloying Element, Taylor & Francis Inc, New York, 2002.
[3] R.G. Hamerton, H. Cama, M.W. Meredith, Mater. Sci. Forum 331-337 (2000) 143.
[4] V. Raghavan, JPEDAV. 28 (2007) 192–196.
[5] A.E. Ares, C.E. Schvezov, Metal. Mat. Trans. 38A (2007) 1485-1499.
[6] P. Campestrini, Microstructure-Related Quality of Conversion Coating on Aluminium Alloys, DUP Science, 2002.
[7] T. Savaşkan, O. Bican, Mat. Sci. Eng. 404A (2005) 259–269.
[8] R. Ciach, M. Podosek, J. Therm. Anal. 38(9) (1992) 2077-2085.
[9] D.E.Groteke, In: International Die Casting Congress and Exposition, A Production Filtration Process fo Alumiuium Melts 1983, p.7.
[10] S. Popović, Cryst. Res. Technol. 20 (1985) 552-555.
[11] S. Popović, B.Grzeta, V. Ilakovac, R. Kroggel, G. Wendrock, H. Loffler, Phys. Stat. Sol. 130A (1992) 273- 292.
[12] S. Popović, B. Gržeta, V. Ilakovac, H. Löffler, G. Wendrock, Phys. Stat. Sol. 141A (1994) 43-52.
[13] S. Popović, B. Gržeta, H. Löffler, G. Wendrock, Fizika 4A (1995) 529-538.